References and Notes

1. G. J. Giles, H. W. Moos, W. R. McKinney, *J. Geophys. Res.* **81**, 5797 (1976).
2. H. Weiser, R. C. Vitz, H. W. Moos, A. Weinstein, *Appl. Opt.* **15**, 3123 (1976).
3. T. R. McDonough and N. M. Brice, *Icarus* **20**, 136 (1973).
4. D. F. Strobel, *Rev. Geophys. Space Phys.* **13**, 372 (1975).
5. J. E. Blamont, in *Proceedings of the Saturn Ring Workshop*, F. D. Palluconi and G. H. Pettengill, Eds. (Science Publication 343, National Aeronautics and Space Administration, Washington, D.C., 1973), p. 125; M. Dennefeld, *Int. Astron. Union Symp.* **65**, (1974), p. 471.
6. J. B. Pollack, *Space Sci. Rev.* **18**, 3 (1975).

7. This research was supported under NASA grant NGR 21-001-001. The rocket was prepared and launched by the Sounding Rocket Division of Goddard Space Flight Center, Greenbelt, Maryland.

7 February 1977; revised 6 May 1977

Multistranded Helix in Xanthan Polysaccharide

Abstract. *The extracellular polysaccharide xanthan is shown by electron microscopy to be an unbranched, probably double-stranded fiber 4 nanometers wide and 2 to 10 micrometers long when native. Denaturation yields a single strand only 2 nanometers wide and 0.3 to 1.8 micrometers long. Renatured xanthan shows short unraveled regions with two or three strands arranged in a right-handed twist.*

The extracellular polysaccharide xanthan produced by the microorganism *Xanthomonas campestris* finds extensive use as a viscosity-enhancing agent because of its high-specific viscosity and striking pseudoplasticity (*1*). It is already widely used in foods; in addition, there is a large potential application in chemically enhanced oil recovery (*2*). The primary structure of the polymer was recently shown to consist of a main chain made up of β-(1→4)-linked D-glucose, as in cellulose, but with a 3-sugar side chain attached at C(3) to alternate glucose residues of the main chain (*3*). The side chain is β-D-mannose-(1→4)-β-D-glucuronic acid-(1→2)-α-D-mannose-6-*O*-acetyl. About one-third of the terminal mannose residues bear a pyruvic acid acetal. Because of the glucuronic acid and pyruvate groups, xanthan exhibits many typical polyelectrolyte properties.

The secondary and tertiary structures of xanthan are still largely unknown. X-ray scattering from xanthan fibers of poor crystallinity shows a helix with fivefold symmetry and pitch 4.70 nm (*4*, *5*). The pattern has been tentatively interpreted in terms of a single-stranded structure, but a double-helical model has not been ruled out (*5*). Previous solution studies give strong hints of an ordered native conformation. For example, when dissolved in water of low ionic strength, xanthan exhibits a thermally induced conformational transition between a native, probably rodlike structure and a more flexible denatured conformation. This transition, which was first observed by Jeanes and her co-workers (*6*), has until now been characterized only by viscosity measurements (*6–9*), optical rotation or circular dichroism (*7–10*), and nuclear magnetic resonance (*10*). To elucidate this structural change more fully, we have obtained electron micrographs and molecular filtration chromatograms of native, denatured, and renatured xanthan.

Purified native xanthan was prepared from dried commercial powder or from undried culture broths by methods previously described (*11*). Similar results were obtained whether or not the sample had been dried or precipitated at any time in its history. Denatured xanthan was prepared by heating a dilute solution of the native polymer (in deionized water at *p*H 6 to 7) to 95°C for 15 minutes, then quenching the solution in ice water. The denatured polymer thus obtained exhibited at 5°C optical rotation characteristics of the denatured state at high temperatures (*9*). The optical rotation of such a denatured polysaccharide solution in deionized water remained unchanged for many days at 5°C. However, if a small amount of NaCl (0.01 to 0.04*M*) was added to the denatured sample, the optical rotation immediately returned to that of the native form (*9*). We term this a renatured sample. Strikingly similar salt-dependent thermal denaturation and renaturation occur in triple-standard collagen and double-stranded polynucleotides (*12*). In preparing renatured xanthan samples for electron microscopy, the NaCl was replaced through dialysis by 0.01*M* ammonium acetate, *p*H 7.

Electron micrographs of xanthan were obtained by a novel but simple technique, which involves the use of what we call a reactive carbon substrate. Normally, when one prepares carbon substrates the carbon is evaporated at the lowest convenient pressure, usually about 10^{-6} torr. For our reactive films, however, the carbon was evaporated with 10^{-3} to 10^{-4} torr of air remaining; this is the point at which the carbon begins to spark instead of evaporating smoothly. The resulting carbon films have carboxyl, phenol, keto, and quinone groups incorporated in the film's surface. These groups act as reactive sites for the deposition of the polysaccharide.

A microdrop of a solution with a xanthan concentration of 6 parts per million was placed in the center of a standard electron microscope grid covered with the carbon film and allowed to dry in the air of a dust-free, laminar-flow hood. Ap-

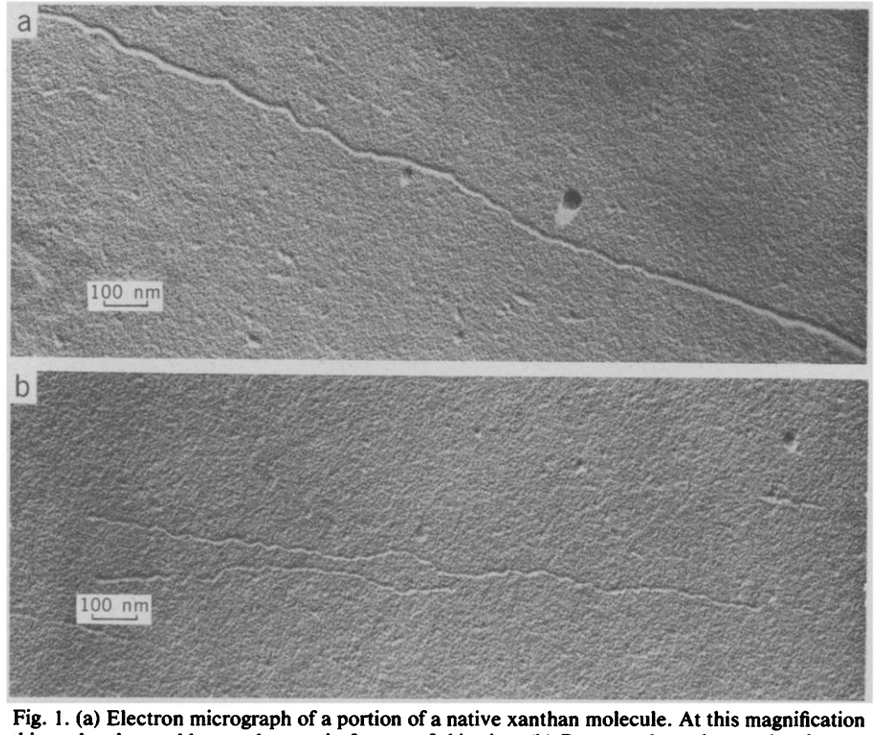

Fig. 1. (a) Electron micrograph of a portion of a native xanthan molecule. At this magnification this molecule would extend over six frames of this size. (b) Denatured xanthan molecules.

parently, as the drop dried the polymer attached itself to the reactive carbon film; the surface tension of the receding drop then caused it to stretch out. This action produced an area around the periphery of the drop in which individual xanthan molecules were stretched out radially. When the dried specimen was then shadowed, there were always two positions around the drop where the molecules lay perpendicular to the direction of shadow. In our work we lightly shadowed with uranium at an angle corresponding to $\tan^{-1}$ (1/4).

The shadowed preparations were examined with a Philips EM 300 high-resolution electron microscope having a resolution better than 0.3 nm. Magnification calibration of the micrographs was obtained from the measurement of spacings of the Ti_4O_7 lattice and is considered accurate to ± 3 percent.

Electron micrographs of native and denatured xanthan are shown in Fig. 1. The native molecule (Fig. 1a) was found to be 2 to 10 μm long, generally smooth, straight, and unbranched, with a thickness of 4 nm in its thickest regions. Denatured molecules (Fig. 1b) were 0.3 to 1.8 μm long, unbranched, and 2 nm thick—half the width of the native molecule. Renatured xanthan, shown in Fig. 2, exhibited fiber lengths equal to or greater than those of the native polymer, as well as a thickness of 4 nm. Although largely unbranched, renatured xanthan showed numerous regions in which the native assembly was partly unraveled. We term such unraveled regions "hockles"; a hockle is apparent in the left end of Fig. 2. The hockles appear to show two or three strands and are arranged in a right-handed twist.

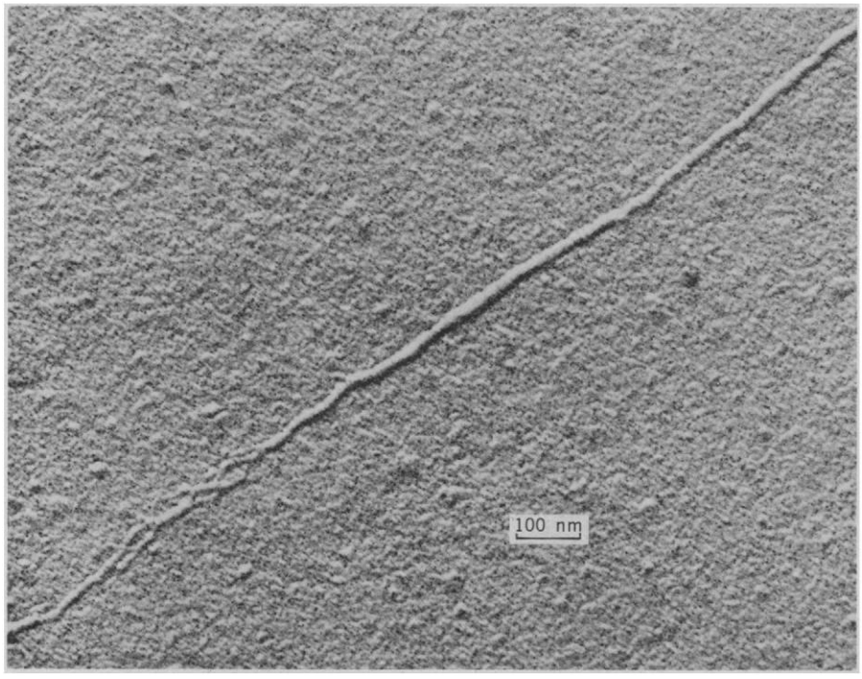

Fig. 2. Electron micrograph of a portion of a renatured xanthan molecule. Note the unraveled strands in the lower left corner.

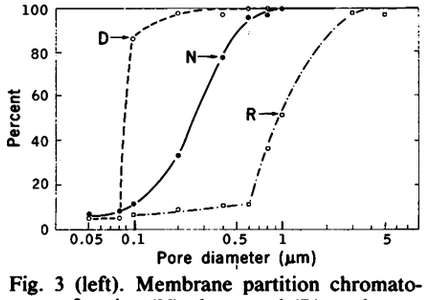

Fig. 3 (left). Membrane partition chromatogram of native (*N*), denatured (*D*), and renatured (*R*) xanthan. The native and denatured molecules were in deionized water at *p*H 7; the renatured molecules were in 0.04*M* NaCl. The xanthan concentration was 0.6 mg/ml and the temperature 0° to 5°C.

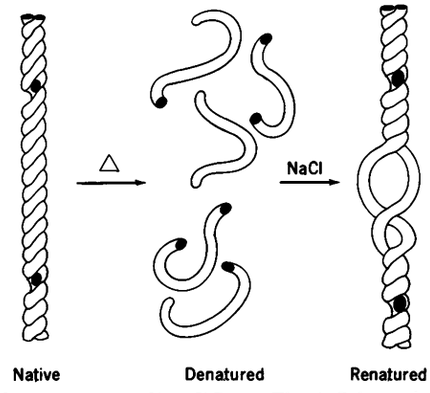

Fig. 4. Schematic representation of the structural changes occurring in the denaturation and renaturation of xanthan. At the left is shown a short section of a native molecule. The two-stranded structure is composed of numerous short individual strands. In the center the individual strands are separated in the denatured form. On the right the strands reassociate to form the renatured assembly. Imperfect reassembly leads to the hockle shown at the center of the renatured molecule. The ratio of chain diameter to chain length is exaggerated for clarity.

Independent evidence for a roughly tenfold change in particle size on denaturation and renaturation is shown by membrane partition chromatograms of the three conformations (Fig. 3). These chromatograms were obtained by pumping a dilute polymer solution at 1 ml/hour through 25-mm-diameter Nuclepore filters of pore diameter 0.05 to 5 μm and analyzing the initial effluent from the filter for carbohydrate by the phenol-H_2SO_4 method (*13*). Only particles of diameter less than the pore size are transmitted by the filter. From Fig. 3 one can see that the native polymer shows a hydrodynamic particle diameter ranging from 0.2 to 0.6 μm. The denatured xanthan exhibits substantially smaller particles; most fall into the narrow range between 0.08 and 0.1 μm. Similarly reduced particle sizes were found for chromatograms of denatured xanthan carried out in distilled water at 75°C. The third curve in Fig. 3 shows that, by contrast, the hydrodynamic diameter of renatured polymer falls between 0.8 and 3 μm, which exceeds even the native polymer's dimensions.

The results presented above demonstrate that the conformational transition native → denatured seen previously by optical activity and viscosity studies is accompanied by the dissociation of a multistranded xanthan assembly, and that renaturation, as seen by optical rotation, is accompanied by a reassociation of strands. Our new observations can be combined into a schematic diagram of the native, denatured, and renatured molecules, as shown in Fig. 4. Because the individual denatured strands are much shorter than the native assembly, many single strands must combine to make up the native structure, as in collagen. The twofold difference in fiber diameter between native and denatured polymers (Fig. 1) suggests that the native molecule is double-stranded, as shown in Fig. 4. However, a triple-stranded structure is not ruled out by these data.

The average molecular weights of native and denatured xanthan can be estimated from their contour lengths as seen in the electron microscope (*14*). For a double-stranded native polymer of con-

tour length 10 μm, the estimated molecular weight is 20×10^6. A denatured single strand of contour length 0.5 μm then has a molecular weight equal to 0.5×10^6. These two results imply that the native molecule is assembled from roughly 40 subunits. The absolute molecular weight of native xanthan has not yet been definitely measured. However, Dintzis and his co-workers (*15*) have measured molecular weights of 1.8 to 3.6×10^6 for xanthan solutions prepared by heating xanthan to 90°C for 3 hours in 4*M* urea. Dispersions of xanthan, in 4*M* urea but not heated, gave molecular weights from light scattering of 11 and 50×10^6 for two different samples (*15*). These experiments provide lower and upper limits to the average molecular weight.

One may ask why the particle lengths in the electron micrographs (Fig. 1) differ by a factor of 10 from the hydrodynamic diameter measured by membrane partition chromatography (Fig. 3). It seems most likely that the xanthan structure is not a rigid rod in solution. Rather, it may behave as a wormlike chain similar to DNA, with a small but finite flexibility which allows substantial coiling up at high molecular weight. Under our method of sample preparation for electron microscopy, these coiled molecules become extended. The intrinsic viscosity of xanthan, 4000 to 7000 ml/g (*9*, *16*), is consistent with this wormlike chain model for molecules with a contour length of 2 to 10 μm.

In summary, our observations demonstrate that native exopolysaccharide from *X. campestris* is composed of many subunit strands 2 nm in diameter arranged in a right-handed double or triple helix or, alternatively, a coiled coil having a diameter of 4 nm. Additional experiments will be required to establish the nature of the interchain association and the place of the 3-sugar side chains in the native and denatured molecules.

G. HOLZWARTH
E. B. PRESTRIDGE
Exxon Research and Engineering Company, Post Office Box 45, Linden, New Jersey 07036

References and Notes

1. A. Jeanes, *J. Polym. Sci. Polym. Symp. No. 45* (1974), p. 209.
2. E. I. Sandvik and J. Maerker, in *Extracellular Microbial Polysaccharides*, P. A. Sandford and A. Laskin, Eds. (American Chemical Society, Washington, D.C., 1977), p. 242; G. J. Hirasaki and G. A. Pope, *Soc. Pet. Eng. J.* **14**, 337 (1974).
3. P. E. Jansson, L. Kenne, B. Lindberg, *Carbohydr. Res.* **45**, 275 (1975); L. D. Melton, L. Mindt, D. A. Rees, G. R. Sanderson, *ibid.* **46**, 245 (1976).
4. R. Moorhouse, M. D. Walkinshaw, S. Arnott, *Abstr. Pap. 171st Meet. ACS* (1976), abstract CELL 097.
5. _____, in *Extracellular Microbial Polysaccharides*, P. A. Sandford and A. Laskin, Eds. (American Chemical Society, Washington, D.C., 1977), p. 90.
6. A. Jeanes, J. E. Pittsley, F. R. Senti, *J. Appl. Polym. Sci.* **5**, 519 (1961).
7. D. A. Rees, *Biochem. J.* **126**, 257 (1972).
8. G. Holzwarth, *Am. Chem. Soc. Div. Pet. Chem. Prepr.* **20** (No. 2), 281 (1976).
9. _____, *Biochemistry* **15**, 4333 (1976).
10. E. R. Morris, in *Extracellular Microbial Polysaccharides*, P. A. Sandford and A. Laskin, Eds. (American Chemical Society, Washington, D.C., 1977), p. 81.
11. Xanthan polysaccharide was obtained from Kelco as a dried powder (keltrol) and as a culture broth. The powder was purified by ultracentrifugation, ethanol precipitation, and dialysis, as previously described (*6*, *9*), to remove cells and other fermentation residues. Culture broth was purified by centrifugation to remove cells and by dialysis to eliminate small molecules and ions; this procedure dispenses with all precipitation and drying steps.
12. W. Traub and K. A. Piez, *Adv. Protein Chem.* **25**, 243 (1971); P. D. Ross and J. M. Sturtevant, *Proc. Natl. Acad. Sci. U.S.A.* **46**, 1360 (1960); F. W. Studier, *J. Mol. Biol.* **41**, 199 (1969).
13. M. Dubois, K. A. Gilles, J. K. Hamilton, P. A. Rebers, F. Smith, *Anal. Chem.* **28**, 350 (1956).
14. X-ray work on xanthan fibers (*4*, *5*) is consistent with a fivefold helix of pitch 4.70 nm, which gives a 0.94-nm rise per disaccharide in the main chain. This is quite similar to the rise in cellulose, 1.03 nm. The average molecular weight of a cellobiose unit with its side chain is 936 for the sodium salt of xanthan. This means that the molecular weight per nanometer of contour length must be about 996 for single-stranded fibers, 1992 for double-stranded fibers, and so on.
15. F. R. Dintzis, G. E. Babcock, R. Tobin, *Carbohydr. Res.* **13**, 257 (1970).
16. P. J. Whitcomb, E. J. Ek, C. W. Macosko, in *Extracellular Microbial Polysaccharides*, P. A. Sandford and A. Laskin, Eds. (American Chemical Society, Washington, D.C., 1977), p. 160.
17. We thank J. Ogletree, P. Skiva, and L. Soni for skillful technical assistance and A. I. Laskin for stimulating discussions.

3 March 1977

Bacteria–Plant Cell Surface Interactions: Active Immobilization of Saprophytic Bacteria in Plant Leaves

Abstract. *Fibrillar structures, originating from the plant cell wall in the intercellular spaces of leaves of 'Red Kidney' bean,* Phaseolus vulgaris *L., engulfed a saprophytic bacterium,* Pseudomonas putida, *after its initial attachment to the host walls. Phytopathogenic bacteria,* Pseudomonas phaseolicola *and* Pseudomonas tomato, *did not adhere to the plant cell wall nor were they encapsulated. Bean lectins may be involved in the attachment and encapsulation processes.*

A principle in plant pathology states that pathogenicity is the exception rather than the rule (*1*); plants have defense mechanisms against most microorganisms, and the exception is that pathogens have found ways to circumvent these defenses. One possible defense mechanism would be for a plant to react to "foreign organisms" and immobilize or destroy them. Evidence for such a process was obtained from experiments involving the intromission and subsequent recovery of bacteria from the intercellular spaces of cowpea leaves (*2*). The recovery of pathogenic bacteria was consistently higher than that of saprophytic bacteria. The reduced recovery of saprophytic bacteria occurred within 20 minutes after infiltration, indicating that the saprophytes but not the pathogens were immobilized by a rapid process within the leaves.

We present here evidence that immobilization and encapsulation of a saprophytic bacterium occurs in the intercellular spaces of bean leaves (*Phaseolus vulgaris* L., variety 'Red Kidney'), in contrast to the lack of attachment and encapsulation with pathogens. A related phenomenon has been described in tobacco (*3*, *4*), but the process in beans differs in several important respects from that in tobacco. Preliminary evidence that plant lectins may be involved in the immobilization and encapsulation processes is also presented.

Attached primary leaves of 8-day-old beans grown in a greenhouse were infiltrated with 10^9 bacteria per milliliter by submerging the leaves in the bacterial suspension and applying a vacuum (740 mm-Hg negative pressure) for 2 minutes. *Pseudomonas putida*, a saprophytic bacterium; *Pseudomonas phaseolicola*, a pathogen causing halo blight of beans; and *Pseudomonas tomato*, a pathogen of tomatoes but not of beans, were used in these studies. As the vacuum was released, the suspension moved through the stomata into the intercellular spaces of the leaves. The water-soaked appearance of the leaves disappeared within about 1 hour after incubation in a growth chamber at 24°C, 85 percent relative humidity, and a light cycle of 12 hours per day provided by both fluorescent and incandescent lighting (2.1×10^4 lux). After specified incubation periods from 1 to 30 hours, the leaves were cut into small pieces and fixed with 3 percent glutaraldehyde in 0.1*M* sodium cacodylate buffer (*p*H 7.2) for 4 to 6 hours. The samples were postfixed with 1 percent osmium tetroxide in the same buffer for 2 hours, dehydrated in an ethanol series, and embedded in Spurr's medium (*5*). Thin sections were cut with a diamond knife, stained with uranyl acetate and lead citrate, and observed with an RCA electron microscope.

Attachment of *P. putida* to plant cell walls was observed 1 hour after infil-